https://doi.org/10.5194/bg-2019-291
Preprint. Discussion started: 31 July 2019

Biogeosciences Discussions Open Access EGU

Partitioning of canopy and soil CO_2 fluxes in a pine forests at the dry timberline

Rafat Qubaja[a], Feyodor Tatarinov[a], Eyal Rotenberg[a], and Dan Yakir[a]*

[a] Department of Earth and Planetary Sciences, Weizmann Institute of Science, Rehovot 76100, Israel

**Correspondence:* Dan Yakir; email: dan.yakir@weizmann.ac.il

Abstract

Partitioning carbon fluxes is key to understanding the process underlying ecosystem response to change. This study used soil and canopy fluxes with stable isotopes (^{13}C) and radiocarbon (^{14}C) measurements of a 50-year-old dry (i.e., 287 mm of annual precipitation) pine forest to partition the ecosystem's CO_2 flux into gross primary productivity (GPP) and ecosystem respiration (Re) and soil respiration flux into autotrophic (Rsa), heterotrophic (Rh), and inorganic (Ri) components. On an annual scale, GPP and Re were 655 and 488 g C m^{-2}, respectively, with a net primary productivity (NPP) of 276 g C m^{-2} and carbon-use efficiency (CUE=NPP/GPP) of 0.42. Soil respiration (Rs) made up 60 % of the total ecosystem respiration and was comprised of 24 ± 4 %, 23 ± 4 %, and 13 ± 1 % Rsa, Rh, and Ri, respectively. The contribution of root and microbial respiration to Re increased during high productivity periods, and inorganic sources were more significant components when soil water content was low. Compared to the mean values for 2001-2006 at the same site; Grünzweig et al., 2009), annual Rs decreased by 27 % to the mean 2016 rates of 0.8 ± 0.1 µmol m^{-2} s^{-1}). This was associated with decrease in the respiration Q_{10} values across the same observation by 36 % and 9 % in the wet and dry periods, respectively. Low rates of soil carbon loss combined with relatively high below ground carbon allocation (i.e., 40 % of canopy CO_2 uptake) help explain the high soil organic carbon accumulation and the relatively high ecosystem CUE of the dry forest. This was indicative of the higher resilience of the pine forest to climate change and the significant potential for carbon sequestration in these regions.

Keywords: Carbon balance, Soil respiration, Autotrophic, Heterotrophic, Inorganic flux, Temperature response, Semi-arid ecosystem, Pine forest, Canopy cover, and Soil chamber.

https://doi.org/10.5194/bg-2019-291
Preprint. Discussion started: 31 July 2019

1. Introduction

On a global scale, soil stores over 1,500 Pg of carbon, which is more than the atmosphere and terrestrial plant biomasses combined (Köchy et al., 2015; Le Quéré et al., 2018; Scharlemann et al., 2014). Soil respiration (Rs) from terrestrial ecosystems and the atmosphere constitutes a large part of the terrestrial carbon cycle (Le Quéré et al., 2018), releasing 68–98 Pg C into the atmosphere as CO_2 annually (Adachi et al., 2017; Hashimoto et al., 2015; Zhao et al., 2017). This is far more than fossil fuel emissions by an order of magnitude (Ballantyne et al., 2015).

The annual net storage of carbon in land biospheres, known as net ecosystem production (NEP), is the balance between carbon uptake during gross primary productivity (GPP), carbon loss during growth and maintenance respiration by plants (i.e., autotrophic respiration [Ra]), and decomposition of litter and soil organic matter (i.e., heterotrophic respiration [Rh]; Bonan, 2008; Chapin et al., 2006; Schulze, 2006). The difference between GPP and Ra is expressed as net primary production (NPP) and is the net carbon uptake of plants used for new biomass production. Measurements from a range of ecosystems have shown that total plant respiration can be as much as 50 % of GPP (Ryan, 1991), and together with Rh comprises total ecosystem respiration (Re, Re = Ra + Rh). The partitioning of ecosystem carbon fluxes can therefore be summarized as:

$$\mathrm{GPP} = \mathrm{NPP} + \mathrm{Ra} = \mathrm{NEP} + \mathrm{Rh} + \mathrm{Ra}. \quad (1)$$

Earlier campaign-based measurements carried out by Maseyk et al. (2008a) and Grünzweig et al. (2009) in the semi-arid *Pinus halepensis* (Aleppo pine) Yatir forest indicated that GPP at this site was lower than that among temperate coniferous forests (1000–1900 g C m^{-2} y^{-1}) but within the range estimated for Mediterranean evergreen and boreal coniferous forests (Falge et al., 2002) with high carbon-use efficiency of 0.4 (CUE = NPP/GPP; DeLucia et al., 2007). The total flux of CO_2 released from the ecosystem (Re) is partitioned into aboveground autotrophic respiration (i.e., through foliage and sapwood [Rf]) and soil CO_2 flux (Rs). Rs, in turn, is a combination of three principal components and can be further partitioned into the components originating from roots or rhizospheres and mycorrhizas (i.e., belowground autotrophic [Rsa]), from carbon respired during the decomposition of dead organic matter by soil microorganisms and macrofaunal (heterotrophic respiration [Rh]; Bahn et al., 2010; Kuzyakov, 2006; Ryan and Law, 2005), and from pedogenic or anthropogenic acidification of soils containing $CaCO_3$ (Ri; Heinemeyer et al., 2007; Kuzyakov, 2006), which is expressed as

https://doi.org/10.5194/bg-2019-291
Preprint. Discussion started: 31 July 2019

$$Re = Rs + Rf = [Rsa + Rh + Ri] + Rf \quad (2)$$

Previously published results show that Rsa contribution to Rs ranges from 24–65 % in forest soils in different biomes and ecosystems (Andersen et al., 2005; Binkley et al., 2006; Chen et al., 2010; Frey et al., 2006; Johnsen et al., 2007; Hogberg et al., 2009; Olsson et al., 2005; Subke et al., 2011). However, most of these experiments were performed in boreal, temperate, or subtropical forests, and there is a general lack of information on water-limited environments, such as dry Mediterranean ecosystems.

The link between soil CO_2 efflux and respiration is complex. For example, a considerable fraction of the respired CO_2 can be dissolved in soil water, transported in hydrological systems, or take part in reactions of carbonate systems. In a calcareous soil with a pH of ~8, most system carbon is bicarbonate (HCO_3^-), while in calcareous soils, CO_2 can be consumed during calcium–carbonate dissolution reactions or released during reverse reactions as carbonate precipitation (Benavente et al., 2010; Cuezva et al., 2011; Kowalski et al., 2008). Processes within root CO_2 can be dissolved in xylem water and carried upward through the transpiration stream (Aubrey and Teskey, 2009; Bloemen et al., 2014).

Soil carbon in semi-arid regions may be strongly influenced by soil inorganic carbon (SIC; Schlesinger, 1982). Its dissolution (which creates a sink for atmospheric CO_2) deposition (i.e., source), or recycling can contribute to soil CO_2 fluxes. On annual to decadal time scales, this contribution is assumed to be marginal at 3–4 g C m^{-2} y^{-1}, compared to 60 ± 6 g C m^{-2} y^{-1} for tundra and up to 1260 ± 57 g C m^{-2} y^{-1} for tropical moist forests (Raich and Schlesinger, 1992). This small abiotic flux can be accepted as an insignificant source compared to biotic CO_2 sources. However, uncertainties concerning the significance of the abiotic process for C budgets in dry ecosystems with calcareous soils exist.

Rates of Rs, have been altered due to global climatic change, particularly through changes in soil temperature (Ts) and soil moisture (SWC; Bond-Lamberty and Thomson, 2010; Buchmann, 2000; Carvalhais et al., 2014; Davidson et al., 1998; Zhou et al., 2009), which account for 65–92 % of the variability of Rs in a mixed deciduous forest (Peterjohn et al., 1994). CO_2 efflux generally increases with increasing soil temperatures (Frank et al., 2002) and can produce positive feedback for climate warming (Conant et al., 1998), converting a biosphere from a net carbon sink to a carbon source (IPCC-AR5 2014). A range of empirical models have been developed to relate Rs rate and temperature (Balogh et al., 2011; Lellei-Kovács et al., 2011), and the most widely used model relies on the Q_{10} approach (Bond-Lamberty and Thomson, 2010), which quantifies the sensitivity of Rs to temperature and integrates physical processes, such as rate of O_2 diffusion into and CO_2 diffusion out of soils and the intrinsic temperature

https://doi.org/10.5194/bg-2019-291
Preprint. Discussion started: 31 July 2019

dependency of enzymatic processes (Davidson and Janssens, 2006). Soil moisture (SWC) may be of greater importance than temperature in influencing Rs in water-limited ecosystems (Cable et al., 2011; Grünzweig et al., 2009; Shen et al., 2008; Saleska et al., 1999). In general, the Rs rate increases with the increase of SWC at low levels but decreases at high levels of SWC (Deng et al., 2012; Hui and Luo, 2004; Jiang et al., 2013). Several studies have connected the sensitivity of carbon fluxes in semi-arid Mediterranean ecosystems to the irregular seasonal and interannual distribution of rain events (Poulter et al., 2014; Ross et al., 2012). While Rs is generally constrained by low SWC during summer months, abrupt and large soil CO_2 pulses have been observed after rewetting dry soil (Matteucci et al., 2014).

Partitioning ecosystem CO_2 fluxes using stable isotopes has been proposed as a powerful partitioning approach (Ogee et al., 2004; Yakir and Sternberg, 2000). Earlier studies in the semi-arid Yatir forest indicated that using ^{13}C creates net ecosystem carbon losses in summer, which are driven by soil emission (Maseyk et al., 2008a), and that different sources of soil carbon can be identified (Grünzweig et al., 2007). Using both ^{13}C and CO_2/O_2 ratios also showed that abiotic processes, such as CO_2 storage, transport, and interactions with sediments, can influence Rs measurements at this site (Angert et al., 2015; Carmi et al., 2013). The current research provides follow-up measurements to the 2001-2006 study at the same site to identify long-term temporal changes in the soil–atmosphere CO_2 fluxes in this environment. It also extends the earlier studies by using continuous soil and ecosystem flux measurements and auxiliary analyses to fully and quantitatively partition soil CO_2 to better understand the high carbon sequestration potential in this semi-arid forest planation, and.

2. Materials and methods

2.1. Site description

The Yatir forest (3˚20' N, 35˚03' E) is located in the transition zone between sub-humid and arid Mediterranean climates (Fig. S1) on the edge of the Hebron mountain ridge at a mean altitude of 650 m. The ecosystem is a semi-arid pine afforestation established in the 1960s and covering approximately 18 km^2. The average air temperatures for January and July are 10 ºC and 25.8 ºC, respectively. Mean annual potential evapotranspiration (ET) is 1,600 mm, and mean annual precipitation is 285 mm. Only winter (December to March) precipitation occurs in this region, creating a distinctive wet season, while summer (June to October) is an extended dry season. There are short transition periods between seasons, with a wetting season (i.e., autumn) and a drying season (i.e., spring). The forest is dominated by Aleppo pine (*Pinus halepensis*), with smaller proportions of other pine species and cypress and little understory

https://doi.org/10.5194/bg-2019-291
Preprint. Discussion started: 31 July 2019

vegetation. Tree density in 2007 was 300 trees ha^{-1}; mean tree height was 10 m; and native background vegetation was sparse shrubland with a total vegetation height of 0.30–0.50 m (Grünzweig et al., 2003).

The soil at the research site is shallow (20–40 cm) Aeolian-origin loess with a clay-loam texture (31% sand, 41 % silt, and 28% clay; density: 1.65 ± 0.14 g cm^{-3}) overlying chalk and limestone bedrock. Deeper soils (up to 1.5 m) are sporadically located at topographic hollows. While the natural rocky hill slopes in the region are known to create flash floods, the forested plantation reduces runoff dramatically to less than 5% of annual rainfall (Shachnovich et al., 2008). Groundwater is deep (> 300 m), reducing the possibility of groundwater recharge due to negative hydraulic conductivity or of water uptake by trees from the groundwater.

2.2. Flux and meteorological measurements

An instrumented eddy covariance tower was erected in the geographical center of Yatir forest, following the EUROFLUX methodology (Aubinet et al., 2000). The system uses a three-dimensional (3D) sonic anemometer (Omnidirectional R3, Gill Instruments) and a closed path LI-COR 7000 CO_2/H_2O gas analyzer (LI-COR Inc., Nebraska, USA) to measure the evapotranspiration flux (ET) and net CO_2 flux (NEE). EC flux measurements were used to estimate the annual scale of NEP by integrating half-hour NEE values. The 15-year NEE record was obtained after U* night-time correction, gap filling, and quality control as described in Tatarinov et al. (2016). A site-specific algorithm was used for flux partitioning into Re and GPP. Daytime ecosystem respiration (Re-d, in µmol m^{-2} s^{-1}) was estimated based on measured night-time (i.e., when the global radiation was < 5 W m^{-2}) values (Re-n), averaged for the first three half-hours of each night. The daytime respiration for each half-hour was calculated according to Eq. 3 (Maseyk et al., 2008a; Tatarinov et al., 2016),

$$R_{e-d} = R_{e-n}(\alpha_1\beta_s^{dT_s} + \alpha_2\beta_w^{dT_a} + \alpha_3\beta_f^{dT_a}) \quad (3)$$

where βs, βw, and βf are coefficients that correspond to soil, wood, and foliage, respectively; dTs and dTa are soil and air temperature deviations from the values at the beginning of the night; and α1, α2, and α3 are partitioning coefficients fixed at 0.5, 0.1, and 0.4, respectively. The βs, βw, and βf coefficients were calculated as follows: βs = 2.45 for wet soil (i.e., soil water content in the upper 30 cm above 20% vol); βs = 1.18 for dry soil (i.e., based on Q_{10} from the Grünzweig et al. [2009] study at the same site); βf = 3.15–0.036Ta; and βw = 1.34 + 0.46 exp (-0.5((DoY-162)/66.1)^2), where DoY is the day of the hydrological year

https://doi.org/10.5194/bg-2019-291
Preprint. Discussion started: 31 July 2019

149 starting from October first. Finally, GPP was calculated as GPP = NEE-Re. Negative values of the NEE
150 and GPP indicated that the ecosystem was a CO_2 sink.

151 Half-hour auxiliary measurements used in this study included photosynthetic activity radiation (PAR mol
152 m^{-2} s^{-1}), vapor pressure deficit (VPD, kPa), wind speed (m s^{-1}), and relative humidity (RH, %)— additional
153 measurements are described elsewhere (Tatarinov et al., 2016). Air temperature (Ta, °C), relative humidity
154 (RH, %), and soil temperature (Ts, °C) were also measured and calculated using soil chambers 20 cm above
155 the soil surface and at a 5 cm depth. These were located at 21 points and measured every half hour using
156 soil chamber system (LI8150-203, LI-COR Lincoln, NE). Volumetric soil water content ($SWC_{0\text{-}10}$) was
157 measured in the upper 10 cm of the soil very half hour near the chambers using the ThetaProbe model
158 ML2x (Delta-T Devices Ltd., Cambridge, UK) calibrated to the soil composition based on the
159 manufacturer's equations.

160 **2.3. Soil CO_2 flux**

161 Soil CO_2 flux (Rs) was measured using automated non-steady-state systems, 20 cm diameter opaque
162 chambers, and a multiplexer to allow for simultaneous control of several chambers (LI -8150, -8100-101, -
163 8100-104; LI-COR, Lincoln, NE). Precision of CO_2 measurements in chamber air was ±1.5 % of the
164 measurements range (0–20,000 ppm). The chamber closed onto preinstalled PVC collars 20 cm in diameter,
165 inserted 5 cm into the soil and 6 cm above the surface, allowing for short measurement times (i.e., 2 min).
166 When measurements were not being taken, chambers were positioned away from collars. Data were
167 collected using a system in which air from the chamber was circulated (2.5 l min^{-1}) through an infrared gas
168 analyzer (IRGA) to record CO_2 (µmol CO_2/mol air) and H_2O (mmol H_2O/mol air) concentrations in the
169 system logger (1 s^{-1}).

170 The rates of soil CO_2 flux or Rs were calculated from chamber data using a linear fit of change in the water-
171 corrected CO_2 mole fraction and Eq. 4 (LiCor Manual, 2015) as follows:
172
173 $$R_s = \frac{dC}{dt} \cdot \frac{v\,P}{s\,T_a R} \quad . \qquad (4)$$
174

175 Here, Rs is the soil CO_2 flux (µmol CO_2 $m^{-2}s^{-1}$), dC/dt is the rate of change in the water-corrected CO_2 mole
176 fraction (µmol CO_2 mol^{-1} air s^{-1}), v is the system volume (m^3), P is the chamber pressure (Pa), s is the soil
177 surface area within the collar (m^2), Ta is the chamber air temperature (K), and R is the gas constant (J mol^{-}

https://doi.org/10.5194/bg-2019-291
Preprint. Discussion started: 31 July 2019

^{1} K^{-1}). A measurement period of 2 minutes was used based on preliminary tests to obtain the most linear increase of CO_2 in the chambers with the highest R^2.

Soil CO_2 fluxes in the experimental plot were measured between November 2015 and October 2016 with three chambers using 21 collars arranged in seven groups (sites) on a half-hour basis (48 daily records). The three chambers were rotated between the seven sites every 1–2 weeks to cover all sites and to assess spatial and temporal variations.

Upscaling of the collar measurements to plot-scale soil CO_2 flux was carried out by grouping collars based on the distance from trees (Dt) (i.e., under trees [< 1 m from nearest tree; UT], in gaps between trees [1–2.3 m; BT], and open areas [> 2.3 m; OA]). One chamber was measured at each microsite group to estimate the fractional areas (Ø) of the three locations based on mapping the sites according to the distances noted above, which was previously done (Raz-Yaseef et al., 2010).

$$Rs = Rs_{OA} * Ø_{OA} + Rs_{BT} * Ø_{BT} + Rs_{UT} * Ø_{UT} \quad (5)$$

$$Ø_{OA} + Ø_{BT} + Ø_{UT} = 1 \quad (6)$$

The annual scale of Rs was derived from the up-scaled chamber based on daily records (48 half hourly values) of spatial up-scaled Rs. Gap filling of missing data due to technical problems (i.e., 27 % of the data across the study period of 2015–2016) was based on the average diurnal cycle of each month, and such data were averaged to obtain the estimate of the annual scale of Rs.

Estimating the temperature sensitivity of Rs (Q_{10}) was done as described by Davidson and Janssens (2006) using a first-order exponential equation (see also Xu et al., 2015),

$$Rs = ae^{bTs}, \quad (7)$$

where Rs represents the half-hour spatial up-scaled time series of soil respiration flux (μmol m^{-2} s^{-1}), Ts (°C) is soil temperature at a 5 cm depth (up-scaled spatially and temporally using the same method as Rs), and a and b are fitted parameters. The b values were used to calculate the Q_{10} value according to the following equation:

$$Q_{10} = e^{10b}. \quad (8)$$

https://doi.org/10.5194/bg-2019-291
Preprint. Discussion started: 31 July 2019

2.4. Soil CO_2 flux partitioning

Determination of different sources of soil CO_2 efflux was based on linear mixing models (Lin et al., 1999) to estimate proportions for three main sources (autotrophic, heterotrophic, and abiotic), using isotopic analysis of soil CO_2 profiles and soil incubation data from eight campaigns (January to September) during 2016 according to Equations 9–11. Partitioning of the monthly Rs values into components was done using a 3-endmember triangular model for interpreting the $\delta^{13}C$ and $\Delta^{14}C$ values of CO_2 flux; the 3-endmember triangular corners are the autotrophic (Rsa), heterotrophic (Rh), and abiotic (Ri) sources of Rs. The $\delta^{13}C$ and $\Delta^{14}C$ isotope signatures of monthly Rs are located inside the triangle (Fig. S2).

$$\delta^{13}C_{Rs} = f_{sa} * \delta^{13}C_{sa} + f_h * \delta^{13}C_h + f_i * \delta^{13}C_i \quad (9)$$

$$\Delta^{14}C_{Rs} = f_{sa} * \Delta^{14}C_{sa} + f_h * \Delta^{14}C_h + f_i * \Delta^{14}C_i \quad (10)$$

$$1 = f_{sa} + f_h + f_i \quad (11)$$

Here, f indicates the fraction of total soil flux (e.g., $f_h = R_h/Rs$), while subscripts sa, h, and i indicate autotrophic, heterotrophic, and inorganic components, respectively. The three equation systems were used to solve the three unknown f fractions of the total soil flux based on empirical estimates of the isotopic end-members. Additionally, δ^{13} and Δ^{14} are the stable and radioactive carbon isotopic ratios, where $\delta^{13}C = [([^{13}C/^{12}C]_{sample}/[^{13}C/^{12}C]_{refrence}) - 1] * 1000‰$, referencing the Vienna international standard (VPDB). Radiocarbon data are expressed as $\Delta^{14}C$ in parts per thousand or per mil (‰), which is the deviation of a sample $^{14}C/^{12}C$ ratio relative to the OxI standard in 1950 (see Taylor et al., 2015), that is $\Delta^{14}C = [([^{14}C/^{12}C]_{sample}/(0.95 * [^{14}C/^{12}C]_{refrence} * \exp[(y - 1950)/8267])) - 1] * 1000‰$, where y is the year of sample measurement.

The $\delta^{13}C_{Rs}$ was estimated monthly using the Keeling plot approach (Figs. S3 and 4; Pataki et al., 2003; Taneva and Gonzalez-Meler, 2011). Soil air was sampled using closed-end stainless steel tubes (6 mm diameter) perforated near the tube bottom at four depths (30, 60, 90, and 120 cm). Samples of soil air were collected in pre-evacuated 150 mL glass flasks with high-vacuum valves, with the dead volume in the tubing and flask necks purged with soil air using a plastic syringe equipped with a three-way valve. The $\delta^{13}C_{sa}$ end-member was estimated based on incubations during the sampling periods of excised roots following Carbone et al. (2008). Fine roots (< 2 mm diameter) were collected, rinsed with deionized water, and incubated for 3 hours in 10 mL glass flasks connected through Swagelok Ultra-Torr tee fittings to 330

https://doi.org/10.5194/bg-2019-291
Preprint. Discussion started: 31 July 2019


Biogeosciences Discussions Open Access EGU

239 mL glass flasks equipped with Louwers high-vacuum-valves. The flasks were flushed with CO_2-free air at
240 room temperature close to field conditions. The CO_2 was allowed to accumulate to at least 2000 ppm (~2
241 h).

242 The heterotrophic ($\delta^{13}C_h$) end-member was estimated as in Taylor et al. (2015), and similar to the root-
243 incubation experiment, soil samples from the top 5 cm of the litter layer or 10 cm below the soil surface
244 were collected, and roots were carefully removed to isolate heterotrophic components. Root-free soils were
245 placed in 10 mL glass flasks and allowed to incubate for 24 hours before being transferred to evacuated
246 330 mL glass flasks. The inorganic source ($\delta^{13}C_i$) end-member was estimated using one gram of dry soil
247 ground to pass through a 0.5 mm mesh placed in a 10 mL tube with a septum cap; then, 12 mL of 1M HCl
248 was added to dissolve the carbonate fraction, and the fumigated CO_2 withdrawn from each tube was
249 collected using a 10 mL syringe and injected into a 330- mL evacuated flask for isotopic analysis.

250 Radiocarbon estimates were based on the work of Carmi et al. (2013) at the same site, adjusted to the
251 measured atmospheric ^{14}C values during the study period (49.5 ‰; Carmi et al., 2013). The $\Delta^{14}C_{sa}$ and
252 $\Delta^{14}C_h$ end-members were estimated based on the assumption that they carry the ^{14}C signatures of 4 and 8.5
253 years, respectively, older than the ^{14}C signature of the atmosphere at the time of sampling, based on mean
254 ages previously estimated (Graven et al., 2012; Levin et al., 2010; Taylor et al., 2015). $\Delta^{14}C_i$ was obtained
255 from Carmi et al. (2013; Table 2). Monthly values of $\Delta^{14}C_{Rs}$ were obtained using the linear equation of the
256 regression line of the measured $\delta^{13}C$ values of Rsa, Rsh, and Ri and the corresponding estimated $\Delta^{14}C$
257 values (Fig. S2) and monthly $\delta^{13}C$ values of Rs.

258 **2.5. Isotopic analysis**

259 Isotopic analysis followed the methodology described in Hemming et al. (2005). The $\delta^{13}C$ of CO_2 in the air
260 was analyzed using a continuous flow mass spectrometer connected a 15-flask automatic manifold system.
261 An aliquot of 1.5 mL of air was expanded from each flask into a sampling loop on a 15-position valve
262 (Valco Houston, TX, USA). CO_2 was cryogenically trapped from the air samples using helium as a carrier
263 gas; it was then separated from N_2O with Carbosieve G (Sigmaaldrich) packed column at 70°C and analyzed
264 on a Europa 20-20 Isotope Ratio Mass Spectrometer (Crewe, UK). $\delta^{13}C$ results were quoted in parts per
265 thousand (‰) relative to the VPDB international standard. The analytical precision was 0.1 %. To measure
266 CO_2, an additional 40.0 mL sub-sample of air from each flask was expanded into mechanical bellows and
267 passed through an infrared gas analyzer (LICOR 6262; Lincoln, NE, USA) in an automated system. The

https://doi.org/10.5194/bg-2019-291
Preprint. Discussion started: 31 July 2019

precision of these measurements was 0.1 ppm. Flasks filled with calibrated standard air were measured with each batch of 10 sample flasks; five standards were measured per 10 samples for $\delta^{13}C$ analyses and four standards per 10 samples for CO_2 analyses.

Organic matter samples were dried at 60°C and milled using a Wiley Mill fitted with size 40 mesh, and soil samples were ground in a pestle and mortar. Soils containing carbonates were treated with M hydrochloric acid. Between 0.2 and 0.4 mg of each dry sample were weighed into tin capsules (Elemental Microanalysis Ltd., Okehampton, UK), and their $\delta^{13}C$ was determined using an elemental analyzer linked to a Micromass Optima IRMS (Manchester, UK). Three replicates of each sample were analyzed, and two samples of a laboratory working standard cellulose were measured for every 12 samples. Four samples of the acetanilide (Elemental Microanalysis Ltd.) international standard were used to calibrate each run, and a correction was applied to account for the influence of a blank cup. The precision was 0.1%.

2.6. Total below ground carbon allocation (TBCA)

TBCA (g C m^{-2} y^{-1}) was calculated following Giardina and Ryan (2002) for the study year (2015–2016) as follows,

$$TBCA = Rs - Rl + \Delta C_{soil}\,, \quad (12)$$

where R_l is the annual above ground litter production from 2014–2015, and ΔC_{soil} is the annual change in below ground total soil organic C. Litter production, not measured during the present study, was estimated based on values obtained by Masyk et al. (2008b) for 2000–2006 (56 g C m^{-2} y^{-1}) assumed to have increased in the study period (2014–2015) proportionally to the measured increase in leaf area index (LAI; 1.31 to 1.9; i.e., R_l = [(1.9*56)/1.31 = 83 g C $m^{-2}y^{-1}$]) and herbaceous litter production. Three plots of 25 m^2 were randomly selected in 2002 and harvested at the end of the growing season, at which time total fresh biomass was weighed and subsamples were used to determine dry weight and C content. Grünzweig et al. (2007) found that herbaceous litter production was close to the average rainfall for the specific year. This method was adapted in the current study for the period between 2014 and 2015. Since above ground litter (Rl; the sum of tree litter and herbaceous litter production) of a given year was mainly produced during that year but decayed during the following hydrological year, TBCA was the current year's Rs and previous year's Rl. ΔC_{soil} was set to constant as the average annual below ground carbon increase since afforestation (Qubaja et al., unpublished).

https://doi.org/10.5194/bg-2019-291
Preprint. Discussion started: 31 July 2019

298 **2.6. Statistical analyses**

299 A paired t-test was used to detect significant differences in Rs and metrological parameters between
300 microsites (OA, BT, and UT) with the significance level set at 0.05. Pearson correlation analysis (*r*) was
301 used to detect the correlation between Rs and meteorological parameters.

302 To quantify spatial-temporal variability in Rs, the coefficient of variation (CV %) was calculated as
303
304 $$\mathrm{CV} = \frac{\text{Standard deviation}}{\text{mean}} \times 100\% \,. \qquad (13)$$
305

306 Heterogeneity was considered weak if CV % ≤ 10 %, moderate if 10 % < CV % ≤ 100 %, and strong if CV
307 % > 100 %. All the analyses were performed using Matlab software, version R2017b (MathWorks, Inc.).

308 **3. Results**

309 **3.1. Spatial variations**

310 The spatial variations in Rs across collars and microsites are reported in Table 1 together with other
311 measured variables. The results indicated an overall mean Rs value of 0.8 ± 0.1 μmol m^{-2} s^{-1} with distinct
312 values for the three microsites. Rs was greater at the UT site than at the BT and OA sites by a factor of ~2.
313 The spatial variability among the microsites was also apparent in the Rs daily cycle (Fig. 1), with clear
314 differences between the wet season (November to April), when the UT showed consistently higher Rs
315 values than at other sites by a factor of about 1.6, and the dry season by a factor of about 2.6. Note that the
316 daily peak in Rs remains at mid-day in both the wet and dry seasons. Overall, the 21 collars showed
317 moderate variations (CV = 55 %; Table 1), negative correlations between Rs and distance from trees (Dt; r
318 = 0.6, $p < 0.05$), similar but statistically insignificant correlations between soil and air temperatures (Ts and
319 Ta; r = 0.3), and positive correlations between SWC and relative humidity (RH; r = 0.3 and 0.2,
320 respectively).

https://doi.org/10.5194/bg-2019-291
Preprint. Discussion started: 31 July 2019

Biogeosciences Discussions Open Access EGU

Table 1 | Annual mean of half-hour values across sites (OA, open area; BT, between trees; UT, under tree) and study period, of soil respiration flux rates (Rs) together with the soil water content at 10 cm depth (SWC), minimum distances from nearby tree (Dt), soil temperature at 5 cm depth (Ts), and air temperature (Ta) and relative humidity (RH) at the soil surface; (numbers in parenthesis indicate ±se).

Sites	Points	Rs [µmol m^{-2} s^{-1}]	SWC [x100 m^3 m^{-3}]	Dt [m]	Ts [ºC]	Ta [ºC]	RH [%]
OA	1_1	1.64 (0.02)	16.5 (0.2)	2.9	15.6 (0.1)	15.4 (0.2)	59.7 (0.5)
	2_1	0.72 (0.01)	14.5 (0.3)	3.6	15.9 (0.2)	15.0 (0.2)	58.4 (0.6)
	3_1	1.23 (0.02)	19.3 (0.3)	7.0	20.6 (0.3)	18.2 (0.2)	53.5 (0.5)
	4_1	0.38 (0.01)	11.3 (0.2)	3.0	22.6 (0.2)	20.8 (0.1)	58.9 (0.4)
	5_1	0.38 (0.01)	5.8 (0.0)	3.0	25.5 (0.1)	24.0 (0.1)	43.1 (0.4)
	6_1	0.31 (0.01)	5.7 (0.1)	2.8	30.0 (0.3)	26.2 (0.3)	51.8 (0.9)
	7_1	0.14 (0.01)	6.1 (0.0)	3.5	25.5 (0.2)	23.2 (0.3)	44.5 (0.9)
	Average	**0.68 (0.21)**	**11.3 (2.1)**	**3.7 (0.6)**	**22.3 (2.0)**	**20.4 (1.6)**	**52.8 (2.6)**
	CV [%]	**81 %**	**50 %**	**41 %**	**24 %**	**21 %**	**13 %**
BT	1_2	0.77 (0.01)	10.5 (0.1)	1.8	16.1 (0.1)	15.2 (0.2)	60.5 (0.5)
	2_2	0.88 (0.01)	12.1 (0.2)	1.5	14.8 (0.2)	14.7 (0.2)	59.5 (0.6)
	3_2	0.84 (0.01)	20.4 (0.3)	2.7	20.1 (0.3)	18.4 (0.2)	54.1 (0.6)
	4_2	0.91 (0.01)	14.4 (0.2)	2.7	23.3 (0.2)	21.3 (0.2)	58.5 (0.4)
	5_2	0.41 (0.00)	3.9 (0.0)	2.0	24.6 (0.1)	24.0 (0.1)	43.2 (0.4)
	6_2	0.41 (0.01)	3.3 (0.1)	2.5	29.1 (0.2)	26.0 (0.3)	52.5 (0.8)
	7_2	0.46 (0.01)	5.5 (0.0)	1.2	23.9 (0.1)	22.8 (0.3)	45.7 (0.9)
	Average	**0.67 (0.09)**	**10.0 (2.4)**	**2.0 (0.2)**	**21.7 (1.9)**	**20.3 (1.6)**	**53.4 (2.6)**
	CV [%]	**35 %**	**63 %**	**29 %**	**23 %**	**21 %**	**13 %**
UT	1_3	1.22 (0.02)	9.3 (0.1)	0.2	15.7 (0.1)	15.2 (0.2)	60.0 (0.5)
	2_3	1.42 (0.01)	14.0 (0.2)	0.3	14.8 (0.2)	14.8 (0.2)	59.4 (0.6)
	3_3	1.64 (0.01)	19.8 (0.3)	0.5	19.0 (0.2)	18.0 (0.2)	54.5 (0.6)
	4_3	1.90 (0.02)	11.3 (0.1)	0.6	22.0 (0.1)	20.8 (0.1)	59.0 (0.4)
	5_3	1.16 (0.01)	4.0 (0.0)	0.4	23.9 (0.1)	23.7 (0.1)	44.1 (0.4)
	6_3	1.29 (0.01)	4.5 (0.1)	0.2	29.5 (0.3)	25.9 (0.3)	52.7 (0.9)
	7_3	0.89 (0.01)	5.2 (0.1)	0.2	25.0 (0.1)	23.0 (0.3)	45.5 (0.9)
	Average	**1.45 (0.13)**	**9.7 (2.2)**	**0.3 (0.1)**	**21.4 (2.0)**	**20.2 (1.6)**	**53.6 (2.5)**
	CV [%]	**25 %**	**60 %**	**46 %**	**25 %**	**21 %**	**12 %**
All	**Average (SE)**	**0.8 (0.1)**	**10 (1)**	**2.0 (0.4)**	**21.8 (1.1)**	**20.3 (0.9)**	**53.3 (1.4)**
	Max	**1.90**	**20**	**7.0**	**30.0**	**26.2**	**60.5**
	Min	**0.14**	**3**	**0.2**	**14.8**	**14.7**	**43.1**
	CV [%]	**55 %**	**55 %**	**82 %**	**23 %**	**20 %**	**12 %**

https://doi.org/10.5194/bg-2019-291
Preprint. Discussion started: 31 July 2019

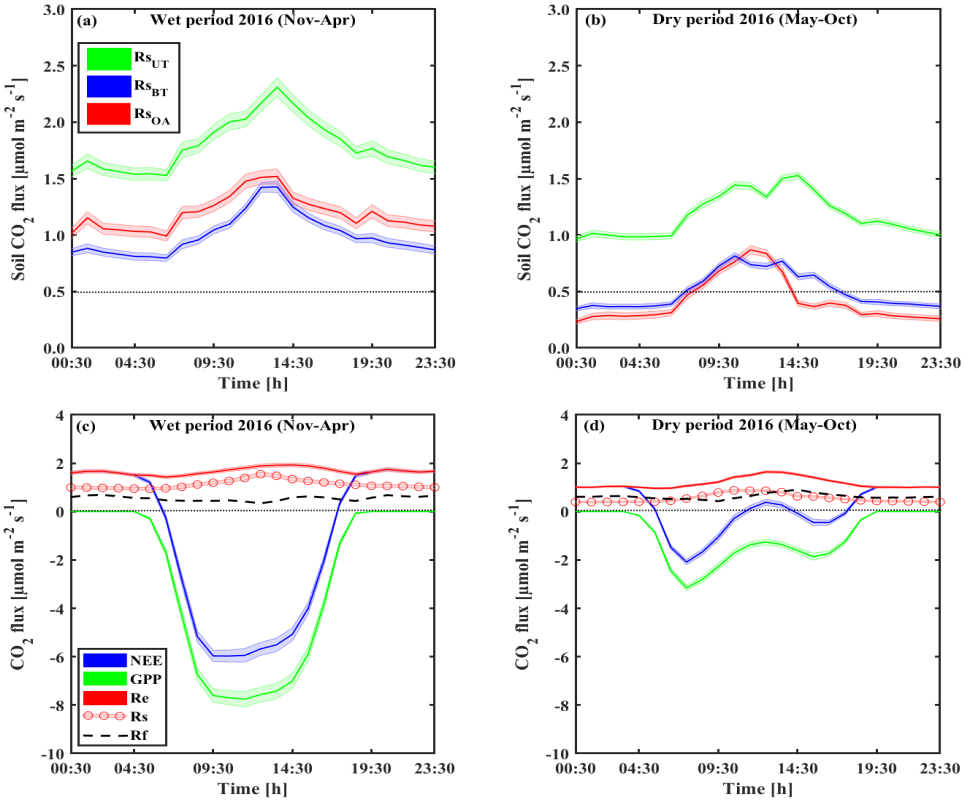

Figure 1 | Representative diurnal cycles of soil respiration (Rs; using soil chambers across microsites: open-area, OA; between-trees, BT; under-trees, UT) in panels a and b, and of net ecosystem exchange (NEE; canopy scale eddy covariance) and gross primary production (GPP), and ecosystem respiration (Re) and its partitioning to soil respiration (Rs) and aboveground tree respiration (Rf) in panels c and d, during the wet (Nov-Apr) and dry (May-Oct) periods. Based on half-hour values over the diurnal cycle; shaded areas indicate ±se; Rf was estimated as the residual as Rf=Re-Rs and was presented as black-dashed line.

3.2. Temporal dynamics

On the diurnal timescale, CO_2 fluxes showed typical daily cycles (Fig. 1). As expected, on average, all CO_2 fluxes were higher during the wet period compared to the dry season by a factor of ~2. However, Rs and Re peaked around mid-day in both the wet and dry seasons, while the more physiologically controlled NEE and GPP showed a shift from mid-day (around 11:00–14:00) to early morning (08:00–11:00) in the dry season, with a mid-day depression and a secondary afternoon peak (Fig. 1d).

The temporal variations across the seasonal cycle are reported in Fig. 2 based on monthly mean values, exhibiting sharp differences between the wet and dry seasons. As previously observed in this semi-arid site, all CO_2 fluxes peak in early spring between March and April. The corresponding high-resolution data

https://doi.org/10.5194/bg-2019-291
Preprint. Discussion started: 31 July 2019

are reported in Fig. S5 and show that in high winter (February), Rs rates were associated with clear days when photosynthetic active radiation (PAR) increased with air temperature Ta. These data also show that following rainy days, daily Rs values could reach 6.1 µmol m^{-2} s^{-1}, although the average was 1.1 ± 0.2 µmol m^{-2} s^{-1} during the wet period, which diminished by ~55 % in the dry season to mean daily values of 0.5 ± 0.1 µmol m^{-2} s^{-1}. In spring (April), all CO_2 fluxes peaked during the crossover trends of decreasing soil moisture content, and increasing temperature, and PAR (Fig. S5).

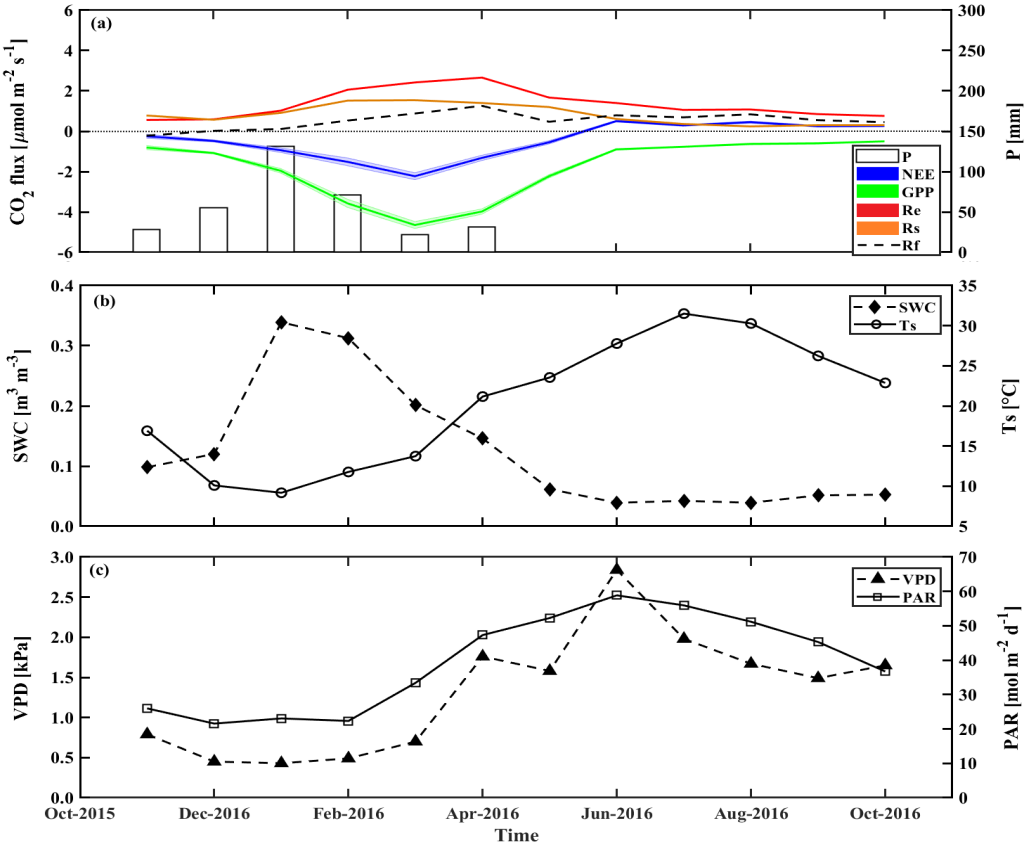

Figure 2| Seasonal trends of monthly mean values during the research period of a) the fluxes of net ecosystem exchange (NEE), gross primary production (GPP), and ecosystem respiration (Re) and its components soil respiration (Rs) and aboveground tree respiration (Rf); and monthly mean of key environmental parameters, b) soil water content at the top 10 cm ($SWC_{0\text{-}10}$) and soil temperature at 5 cm (Ts), and c) vapor pressure deficit (VPD) and photosynthetic activity radiation (PAR). Rf is obtained from the Re-Rs.

The temporal variations in the half-hour values of Rs reflected changes in soil moisture at 0–5 cm depth and PAR (r = 0.5 and 0.2, respectively; $p < 0.01$) and negative correlations with Ts and RH (r = 0.2 and 0.1, respectively; $p < 0.01$). The variations in the integrated Rs showed a CV of 71%, with the temporal

https://doi.org/10.5194/bg-2019-291
Preprint. Discussion started: 31 July 2019

variations dominated by PAR (CV > 100 %) and moderately affected by SWC (CV ~ 85 %), Ts, and RH (CV ~ 40 %). Repeating the models applied by Grünzweig et al. (2009), the potential climatic factors that best predicted daily Rs shifted from SWC and PAR in the dry season to Ts and PAR in the wet season (Table S2). These equations explained 43 % and 70 % of the variation in Rs in the dry and wet seasons, respectively (Table S2). A reasonable forecast of the temporal variations in Rs at half-hour values (R^2 = 0.60, $p < 0.0001$) were obtained based on $SWC_{0\text{-}10}$ and Ts values across the entire seasonal cycle based on:

$$\mathrm{Rs}(\mu\mathrm{mol\ m^{-2}\ s^{-1}}) = 0.05126 * \exp(0.04274 * \mathrm{Ts} + 28.51 * \mathrm{SWC} - 74.44 * \mathrm{SWC}^2). \quad (14)$$

At the ecosystem scale, Re was characterized by high fluxes in the wet season and peak values of ~2.4 µmol m^{-2} s^{-1} in February to April (Fig. 2; Table S1). Refluxes rapidly decreased after rainy cessation and reached the lowest values in the fall (SeptemberOctober) with mean dry period values of 0.5 ± 0.1 µmol m^{-2} s^{-1} (Fig. 2, Table S1). GPP had a mean value of -1.8 ± 0.4 µmol m^{-2} s^{-1}, and daily NEE had a mean value of -0.5 ± 0.3 µmol m^{-2} s^{-1} (Table S1 and Fig. S5), with the same seasonality (Fig. 2).

Table 2 | $\delta^{13}C$ and $\Delta^{14}C$ signature of soil respiration (Rs) and its partitioning to autotrophic (Rsa), heterotrophic (Rh), and the abiotic (Ri), together with the relative contribution of each to the soil and ecosystem respiration for Yatir forest during 8 campaigns of measurements from January to September 2016 (numbers in parenthesis indicate ±se). The monthly contribution of Rsa, Rh, and Ri to Rs or Re are presented in Fig. 3a and b, respectively.

Signature	Rsa	Rh	Ri	Rs
	[‰]			
$\delta^{13}C$	-23.7 (0.5)[1]	-24.3 (0.0)[1]	-6.5 (0.0)[1]	-20.8 (±0.6)[1]
$\Delta^{14}C$	30[3]	50[3]	-900[2]	-134 (34)[4]
Relative contribution to Rs	**0.40 (0.02)**	**0.39 (0.02)**	**0.21 (0.04)**	
Relative contribution to Re	**0.24 (0.04)**	**0.23 (0.04)**	**0.13 (0.01)**	**0.60 (0.06)**

[1] Measured at the present study.
[2] Measured by Carmi et al., (2013).
[3] Calculated based on the measured atmospheric value by Carmi et al., (2013).
and [4] Calculated based on the best fit regreeion equation in Figure S2.

Figure 3 (see also Table 2) summarizes the seasonal variations in Rs and Re partitioning. The monthly Rsa and Rh were not significantly different but were significantly different from Ri ($p < 0.05$). The Rsa/Rs ratios ranged from 0.32 to 0.46, with the largest contribution in early spring from Februaryto–April. The Rh/Rs fraction ranged between 0.33 and 0.45, being highest during the wet season. The Ri/Rs fraction of total respiration from inorganic sources ranged from 0.09 to 0.35, with the largest contribution in the driest period. The mean relative contribution of these components to Rs over the sampling campaigns are presented in Figure 3a, but on average, soil biotic fluxes were higher than abiotic fluxes by a factor of ~4. Repartitioning showed an average increase in Rf/Re from 25 % in the wet season to 54 % in the dry season and a decline in Rs/Re from 75 % to 46 % on average in the wet and the dry seasons, which reflected a

https://doi.org/10.5194/bg-2019-291
Preprint. Discussion started: 31 July 2019

seasonal change of Rf in the wet season to peak values in the dry season (Fig. 3b). Both the highest and lowest Rs fractions (~0.74 and nearly 0.34) along the seasonal cycle were associated with low total Re fluxes, that is in the fall before the Rf peak in the spring and in the summer when physiological controls limited water loss.

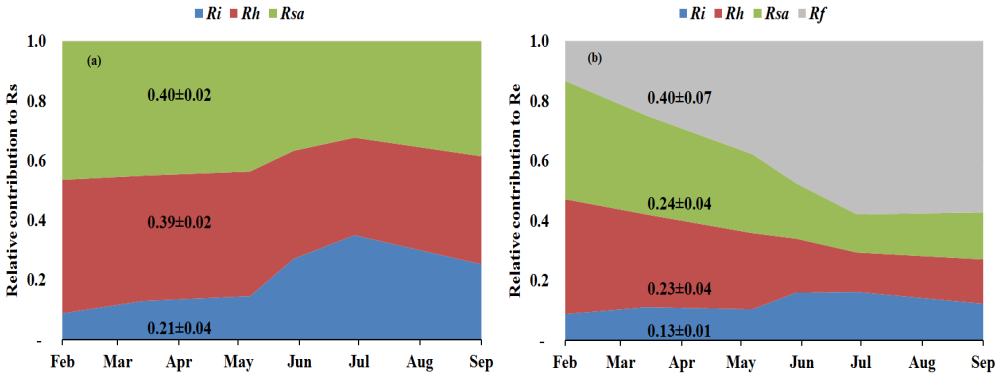

Figure 3 | a) Linear mixing models $\delta^{13}C$ and $\Delta^{14}C$ of soil respiration (Rs) isotope signatures (from soil CO_2 profile method at 0, 30, 60, 90, and 120 cm soil depth) were used to determine the seasonal variations in the relative contribution of soil autotrophic (Rsa), heterotrophic (Rh), and abiotic (Ri) components to Rs, and b) seasonal variations in the relative contribution of soil autotrophic (Rsa), heterotrophic (Rh), abiotic (Ri), and foliage and stem respiration (Rf is obtained from the Re-Rs.) components to ecosystem respiration (Re) during 8 campaigns (Jan-Sep) in 2016. These results confirmed earlier estimates of Grünzweig et al. (2009) and Maseyk et al. (2008a).

3.4. Annual scale

Table 3 | Mean annual values of ecosystem respiration (Re), its components and associated ratios, net ecosystem exchange (NEE; from eddy covariance), net primary productivity (NPP), gross primary productivity (GPP), carbon-use efficiency (CUE), leaf aria index (LAI), and ratio of total belowground Carbon allocation (TBCA) to GPP (TBCA/GPP) in the present study (mean of Nov-2015 to Oct-2016) and in comparison to results obtained previously at the same site (2001-2006 mean values). Ri, Rh, Rsa, Rs, Rl and Rw denote abiotic, heterotrophic, autotrophic, soil, foliage, and wood CO_2 flux, Δ indicates the difference between the mean values for the two studies; using mean values for the two study periods. Q_{10} as derived during the two studies for the wet and dry season.

Study	Ri	Rh	Rsa	Rs	Rl	Rw	Re	NEE	NPP	GPP
					[g m^{-2} y^{-1}]					
Mean (2001-2006)	56	139	211	406	260	70	735	-211	350	-880
x/Re	0.08	0.19	0.29	0.55	0.35	0.10				
x/GPP	0.06	0.16	0.24	0.46	0.30	0.08	0.84	0.24	0.40	
Mean (2015-2016)	61	115	119	295	156	39	488	-167	276	-655
x/Re	0.13	0.23	0.24	0.60	0.32	0.08				
x/GPP	0.09	0.18	0.18	0.45	0.24	0.06	0.75	0.25	0.42	

Study	CUE	Q_{10}		LAI	TBCA/GPP	ΔRf-ratio/ΔLAI	ΔRs-ratio/ΔLAI
		SWC^1	SWC^2	[m^2 m^{-2}]			
Mean (2001-2006)	0.40	2.5	1.2	1.3	0.41		
						-0.05	0.07
Mean (2015-2016)	0.42	1.6	1.1	2.1	0.38		

[1] SWC≥0.2 [m^3 m^{-3}].and [2] SWC<0.2 [m^3 m^{-3}].

https://doi.org/10.5194/bg-2019-291
Preprint. Discussion started: 31 July 2019

On an annual time-scale, estimates of CO_2 flux components based on EC measurements resulted in annual values of GPP, NPP, Re, and NEP of 655, 276, 488, and 167 g C m^{-2} y^{-1}, respectively (Tables 3 and S1). On average across the measurement period, Rs was the main CO_2 flux into atmosphere, making up 60 ± 6% of Re (295 ± 4 g C m^{-2} y^{-1}; Tables 3 and S1), and Rf was another significant component accounting for 40 ± 6% of Re (Fig. 3b), which reflected the low density (300 trees ha^{-1}) nature of the semi-arid forest. As indicated above, Re partitioning showed a decrease in Rs/Re and an increase in Rf/Re from winter to summer, which is clearly apparent in Fig. 3b. On an annual scale, during the study period, estimates of Rf, Rsa, Rh, and Ri values were 194 ± 36, 119 ± 21, 115 ± 20, and 61 ± 6 g C m^{-2} y^{-1}, respectively. Despite relatively high rates of respiration fluxes, the CUE of the ecosystem remained high at 0.42.

Table 4 | Linear regression over time of ecosystem respiration (Re), its components and associated ratios, net ecosystem exchange (NEE; from eddy covariance), net primary productivity (NPP), gross primary productivity (GPP), total belowground Carbon allocation (TBCA), and ratio of TBCA/GPP (2001-2016) in the semi-arid pine forest site. Rh, Rs, and Rf denote heterotrophic, soil, and foliage and wood CO_2 flux. The model parameters (slope and intercept) reported for each variable together with the squared coefficient of regression (R^2) and the *P-value*. The data for the regression analysis includes 15 years (2001-2016) of the site's flux records of Re, NEE, GPP, NPP; and from comparing the data from the earlier 2001-2006 to the present stud (Nov-2015-Oct-2016) for 7 years of Rs, Rh, Rf, and TBCA and TBCA/GPP.

Variables	**Linear regression**			
	Slope	**Intercept**	**R^2**	***P-value***
Re	1.0	386	0.0	0.819
Rs	**-11.0**	**436**	**0.6**	**0.036**
Rh	-3.9	159	0.1	0.404
Rf	-7.1	341	0.3	0.180
NEE	9.0	-231	0.2	0.065
GPP	8.0	-617	0.1	0.254
NPP	-8.8	304	0.2	0.083
TBCA	-9.4	367	0.5	0.114
TBCA/GPP	-0.006	0.43	0.2	0.416

Using the site records of nearly 20 years, long-term trends in GPP, NPP, Re, and NEP were obtained. Comparison of present results with the 2001-2006 values obtained by Grünzweig et al. (2009) and Maseyk et al. (2008a) provided a basis for estimating the temporal trends in soil respiration. Notably, no clear or significant trend over time was observed in any of the canopy-scale fluxes (Table 4). However, the soil respiration rates, Rs, decreased significantly by 11 ± 4 g C m^{-2} y^{-1} (R^2 = 0.62, p = 0.036; Table 4) from regression of the 2001-2006 value to the mean value in the present study (Nov-2015-Oct-2016). Because of strong influenced of variations in environmental conditions, primarily precipitation on interannual variations, it is likely that the relative contributions of the different fluxes, expressed as ratios in Table 3, provide a relatively robust perspective of the long-term temporal changes in the ecosystem functioning. Based on long-term results presented in Table 3, Rf/Re (Rf ratio) decreased by 11 % while Rs/Re (Rs ratio)

https://doi.org/10.5194/bg-2019-291
Preprint. Discussion started: 31 July 2019

increased by 9 % over the observation period noted above (essentially 2003 to 2016). Notably, LAI increased across the same observation period from 1.3 to 2.1 (+57 %; Qubaja et al., unpublished), indicating that the ΔRf-ratio/ΔLAI decreased (-0.05/0.75=-0.07), and the ΔRs-ratio/ΔLAI increased (+0.05/0.75=+0.07; Table 3). These results highlight the shift from Rf to Rs over the 13 years observation period. Total TBCA was 247 g C m^{-2} y^{-1} during the study period and relative below ground partitioning of carbon in the ecosystem (TBCA/GPP) averaged 38%, which was lower than the previous study by 7 % for the same site (Grünzweig et al., 2009).

4. Discussion

Partitioning ecosystem carbon fluxes and long-term observational studies are key to understanding ecosystem carbon dynamics and their response to change. This research hypothesized that soil CO_2 efflux at the dry study site is a key factor underlying the observation of high NEP and high CUE in this system. Comparing CO_2 fluxes in this forest with fluxes in a range of European forests showed that mean NEP in the semi-arid forest (160 g C m^{-2} y^{-1}) was similar to the mean NEP across other European forests (150 g C m^{-2} y^{-1}; FLUXNET). In contrast, soil CO_2 efflux in the semi-arid forest was 295 g C m^{-2} y^{-1}, which is at the low end of Rs values across the range for other climatic regions, from 50 to 2750 g C m^{-2} y^{-1} (Adachi et al., 2017; Bond-Lamberty, 2018; Chen et al., 2014; Grünzweig et al., 2009; Hashimoto et al., 2015). This is clearly lower than the mean Rs value for global evergreen needle forests, which is estimated at 690 g C m^{-2} y^{-1} (Chen et al., 2014), and between estimates for desert scrub and Mediterranean woodland (224–713 g C m^{-2} y^{-1}; Raich and Schelsinger, 1992). The mean rate of Rs, 0.8 µmol m^{-2} s^{-1}, is also in the range reported for unmanaged forest and grassland in the dry Mediterranean region (0.5 and 2.1 µmol m^{-2} s^{-1}; Correia et al., 2012). High productivity associated with low Rs supports the high CUE estimate and the carbon sequestration potential of the semi-arid Aleppo pin plantation (Rotenberg and Yakir, 2010).

The spatial variations in Rs among the microsites (Table 1) can be approximated to estimate the possible impact on Rs caused by changes in forest density associated with a drying climate (e.g., tree thinning and motality). For example, decreasing from the present optimal stand density (Raz-Yaseef et al., 2010) of 300 trees ha^{-1} to 100 trees ha^{-1} would result, based on present results, in decreasing ecosystem Rs and increasing soil evaporation (Es) by 11 % and 38 %, respectively. This is consistent with the trend for increasing stand density (Litton et al., 2004) and the effects of stand density on Rs through effected litterfall, TBCA, and total soil N (Noh et al., 2010). More work is needed to determine the net effects of such changes (see Maseyk et al., 2011; Villegas et al., 2015).

Low Rs values were associated with relatively high rates of autotrophic respiration, with a mean annual-scale Rsa/Rs ratio of 0.40, which is similar to the estimated global mean value within the range of 0.09 to 0.49 (Chen et al., 2014; Hashimoto et al., 2015). Heterotrophic respiration was of the same magnitude

https://doi.org/10.5194/bg-2019-291
Preprint. Discussion started: 31 July 2019

(annual-scale Rh/Rs ratio: 0.39 ± 0.02; Table 2 and Fig. 3), which reflected an increasing trend of +14 % from mean 2001-2006 values (Grünzweig et al., 2009; Maseyk et al., 2008a) to the mean values in the present study. This ratio is lower than the estimated global mean Rh/Rs of 0.56 (Hashimoto et al., 2015) but comparable to the long-term trend of +17 % between 1990 and 2014 (Bond-Lamberty et al., 2018). The seasonal dynamics in Rs partitioning (Fig. 3) might reflect an increasing balance between Rsa and Rh compared to Rsa dominance in the dry season, which was present in the earlier study (Grünzweig et al., 2009; Maseyk et al., 2008a; see also Carbone et al., 2008, Tang et al., 2005).

Carbon partitioning below ground (TBCA/GPP) was relatively high at 0.38, despite a ~7 % decrease in values compared to those reported by Grünzweig et al. (2009) but was similar to the mean value for forests in various biomes (Litton et al., 2007). This explains the high rate of SOC accumulation observed over the period since afforestation (Grünzweig et al., 2007; Qubaja et al., unpublished). The ratio of Rs/GPP did not change over the observation period (0.46 vs. 0.45 for 2001-2006 vs. 2015-2016 mean values) but shifted to a larger contribution of Rh (Table 3).

The relatively low annual scale of the heterotrophic respiration to Rs was consistent with the dry surface soil layer over much of the year in this forest (Figures 2 and S5) and the observed low decomposability of plant detritus and high mean SOC accumulation rate (Grünzweig et al., 2007). The small increase in Rh proportional contribution to Rs may reflect the general climatic trends in the region of increasing temperature, with no significant change in precipitation (Bond-Lamberty et al., 2018).

The relatively low Rs under conditions of high temperature in the semi-arid ecosystem implies reduced to sensitivity of respiration to temperature. This is partly imposed by low SWC conditions during extended parts of the year (Grünzweig et al., 2009; cf. Rey et al., 2002; Xu and Qi, 2001). Accordingly, Rs varied with Ts only under relatively wet conditions, but during 8–9 months of the year when SWC was below a threshold value of 0.2 $m^3 m^{-3}$, Rs varied with water availability. The Rs vs. Ts relationship used to estimate apparent Q_{10} values indicated a decrease from Q_{10} = 1.6 in the wet season to Q_{10} = 1.1 in the dry season. This represents a similar trend in Q_{10} compared to the results of Grünzweig et al. (2009; Table 3). The estimated Q_{10} values are consistent with published values that range from 1.4 to 2.0 among different ecosystems (Hashimoto et al., 2015; Zhou et al., 2009) and with low values under low SWC (Reichstein et al., 2003; Tang et al., 2005). The low temperature sensitivity in the dry season must be related to reduced microbial activity but may also involve down regulation of the plant activity (Maseyk et al., 2008a) and drought-induced dormancy of shallow roots (Schiller, 2000). Little is known about the differences in Q_{10} of soil Rh and Rsa respirations (Yu et al., 2017), which could respond differently to different environmental variables (Matteucci et al., 2015) and make distinct contributions to soil carbon sequestration (Kuzyakov, 2006). Previous studies have shown that Rh and Rsa exhibit different temperature sensitivities (Rey et al.,

https://doi.org/10.5194/bg-2019-291
Preprint. Discussion started: 31 July 2019

2002), but the underlying causes of the temporal changes observed in the Q_{10} values at the study sites in this study remain uncertain.

Dry lands can obtain water from sources other than precipitation, yet little is known about how non-rainfall water influences dry land communities and activity. The results presented here and in previous studies (Agam and Berliner, 2004; Kosmas et al., 1998) show that water vapor adsorption may occur relatively frequently in dry seasons in dry environments. Re-evaporation is proposed to help protect against the effects of extreme drought and to influence other ecosystem processes, such as stimulating microbial activities, litter decomposition, and desert lichen activity (Dirks et al., 2010; Gliksman et al., 2017; Kuehn et al., 2004; Newell et al., 1985; Kappen et al., 1979; Lange et al., 2006). More information on the potential role and importance of water-vapor adsorption in a dry environment is needed.

Net ecosystem CO_2 exchange measurements are usually assumed to be strongly dominated by biological processes (e.g., photosynthesis, respiration, or microbial activities), while the contribution of nonbiological processes, such as those associated with carbonate precipitation and dissolution reactions in calcareous soils, are seldom considered. The relative importance of abiotic component to the CO_2 flux, however, greatly increases in dry environments and in dry seasons when biological activities drastically decrease (Kowalski et al., 2008; Lopez-Ballesteros et al., 2017; Serrano-Ortiz et al., 2010), which includes the observation of enhanced weathering at the present study sites (Roland et al., 2012). Notably, ambiguity exists among the terms ‘source’ and ‘sink’ when considering the CO_2 exchange between carbonate rocks and the atmosphere and carbon sequestration (Eshel et al., 2007). In the present study, carbonate precipitation was on average 9 % of the GPP and 13 % of Re during the study period (Table 3). This demonstrates the importance of this flux in semi-arid systems and its potential influence on estimating short-term Re fluxes (Angert et al., 2015; Roland et al., 2012).

Data availability

The data used in this study are archived and available from the corresponding author upon request (dan.yakir@weizmann.ac.il).

Author contributions

RQ and DY designed the study; RQ, FT, ER and DY performed the experiments. RQ and DY analyzed the data. DY and RQ wrote the paper with discussions and contributions to interpretations of the results from all coauthors.

Competing interests

https://doi.org/10.5194/bg-2019-291
Preprint. Discussion started: 31 July 2019

The authors declare that they have no conflict of interest.

5. Acknowledgements

This long-term study was funded by Forestry department of Keren-Kayemeth-LeIsrael (KKL) and the German Research Foundation (DFG) as part of the project “Climate feedbacks and benefits of semi-arid forests” (CliFF) and by the Israel Ministry of Science and the Ministry of National Education, Higher Education, and Research (MENESR) of France (IMOS-French Program: 3-6735). The authors thank Efrat Schwartz for assistance with lab work. The long-term operation of the Yatir Forest Research Field Site is supported by the Cathy Wills and Robert Lewis Program in Environmental Science. We thank the entire Yatir team for technical support and the local KKL personnel for their cooperation.

6. References

Adachi, M., Ito, A., Yonemura, S., & Takeuchi, W. (2017). Estimation of global soil respiration by accounting for land-use changes derived from remote sensing data. Journal of Environmental Management, 200, 97-104.

Agam, N., & Berliner, P. R. (2004). Diurnal water content changes in the bare soil of a coastal desert. Journal of Hydrometeorology, 5(5), 922-933. doi:10.1175/1525-7541(2004)005<0922:dwccit>2.0.co;2

Andersen, C. P., Nikolov, I., Nikolova, P., Matyssek, R., & Haberle, K. H. (2005). Estimating "autotrophic" belowground respiration in spruce and beech forests: decreases following girdling. European Journal of Forest Research, 124(3), 155-163.

Angert, A., Yakir, D., Rodeghiero, M., Preisler, Y., Davidson, E. A., & Weiner, T. (2015). Using O-2 to study the relationships between soil CO2 efflux and soil respiration. Biogeosciences, 12(7), 2089-2099.

Aubinet, M., Grelle, A., Ibrom, A., Rannik, U., Moncrieff, J., Foken, T., et al. (2000). Estimates of the annual net carbon and water exchange of forests: The EUROFLUX methodology. Advances in Ecological Research, Vol 30, 30, 113-175.

Aubrey, D. P., & Teskey, R. O. (2009). Root-derived CO2 efflux via xylem stream rivals soil CO2 efflux. New Phytologist, 184(1), 35-40.

Bahn, M., Janssens, I. A., Reichstein, M., Smith, P., & Trumbore, S. E. (2010). Soil respiration across scales: towards an integration of patterns and processes. New Phytologist, 186(2), 292-296.

Ballantyne, A. P., Andres, R., Houghton, R., Stocker, B. D., Wanninkhof, R., Anderegg, W., et al. (2015). Audit of the global carbon budget: estimate errors and their impact on uptake uncertainty. Biogeosciences, 12(8), 2565-2584.

Balogh, J., Pinter, K., Foti, S., Cserhalmi, D., Papp, M., & Nagy, Z. (2011). Dependence of soil respiration on soil moisture, clay content, soil organic matter, and CO2 uptake in dry grasslands. Soil Biology & Biochemistry, 43(5), 1006-1013.

Benavente, J., Vadillo, I., Carrasco, F., Soler, A., Linan, C., & Moral, F. (2010). Air Carbon Dioxide Contents in the Vadose Zone of a Mediterranean Karst. Vadose Zone Journal, 9(1), 126-136.

Binkley, D., Stape, J. L., Takahashi, E. N., & Ryan, M. G. (2006). Tree-girdling to separate root and heterotrophic respiration in two Eucalyptus stands in Brazil. Oecologia, 148(3), 447-454.

Bloemen, J., Agneessens, L., Van Meulebroek, L., Aubrey, D. P., McGuire, M. A., Teskey, R. O., et al. (2014). Stem girdling affects the quantity of CO2 transported in xylem as well as CO2 efflux from soil. New Phytologist, 201(3), 897-907.

Bonan, G. B. (2008). Ecological climatology : concepts and applications (2nd ed.. ed.). Cambridge: Cambridge : Cambridge University Press.

Bond-Lamberty, B. (2018). New Techniques and Data for Understanding the Global Soil Respiration Flux. Earths Future, 6(9), 1176-1180.

Bond-Lamberty, B., & Thomson, A. (2010). Temperature-associated increases in the global soil respiration record. Nature, 464(7288), 579-U132.

Bond-Lamberty, B., Bailey, V. L., Chen, M., Gough, C. M., & Vargas, R. (2018). Globally rising soil heterotrophic

https://doi.org/10.5194/bg-2019-291
Preprint. Discussion started: 31 July 2019

583 respiration over recent decades. Nature, 560(7716), 80-+.
584 Buchmann, N. (2000). Biotic and abiotic factors controlling soil respiration rates in Picea abies stands. Soil Biology
585 & Biochemistry, 32(11-12), 1625-1635.
586 Cable, J. M., Ogle, K., Lucas, R. W., Huxman, T. E., Loik, M. E., Smith, S. D., et al. (2011). The temperature
587 responses of soil respiration in deserts: a seven desert synthesis. Biogeochemistry, 103(1-3), 71-90.
588 Carbone, M. S., Winston, G. C., & Trumbore, S. E. (2008). Soil respiration in perennial grass and shrub ecosystems:
589 Linking environmental controls with plant and microbial sources on seasonal and diel timescales. Journal of
590 Geophysical Research-Biogeosciences, 113(G2).
591 Carmi, I., Yakir, D., Yechieli, Y., Kronfeld, J., & Stiller, M. (2013). VARIATIONS IN SOIL CO2
592 CONCENTRATIONS AND ISOTOPIC VALUES IN A SEMI-ARID REGION DUE TO BIOTIC AND
593 ABIOTIC PROCESSES IN THE UNSATURATED ZONE. Radiocarbon, 55(2-3), 932-942.
594 Carvalhais, N., Forkel, M., Khomik, M., Bellarby, J., Jung, M., Migliavacca, M., et al. (2014). Global covariation of
595 carbon turnover times with climate in terrestrial ecosystems. Nature, 514(7521), 213-+.
596 Chapin, F. S., III, Woodwell, G. M., Randerson, J. T., Rastetter, E. B., Lovett, G. M., Baldocchi, D. D., et al. (2006).
597 Reconciling carbon-cycle concepts, terminology, and methods. Ecosystems, 9(7), 1041-1050.
598 Chen, D., Zhang, Y., Lin, Y., Zhu, W., & Fu, S. (2010). Changes in belowground carbon in Acacia crassicarpa and
599 Eucalyptus urophylla plantations after tree girdling. Plant and Soil, 326(1-2), 123-135.
600 Chen, S. T., Zou, J. W., Hu, Z. H., Chen, H. S., & Lu, Y. Y. (2014). Global annual soil respiration in relation to
601 climate, soil properties and vegetation characteristics: Summary of available data. Agricultural and Forest
602 Meteorology, 198, 335-346.
603 Conant, R. T., Klopatek, J. M., Malin, R. C., & Klopatek, C. C. (1998). Carbon pools and fluxes along an
604 environmental gradient in northern Arizona. Biogeochemistry, 43(1), 43-61.
605 Correia, A. C., Minunno, F., Caldeira, M. C., Banza, J., Mateus, J., Carneiro, M., . . . Pereira, J. S. (2012). Soil water
606 availability strongly modulates soil CO2 efflux in different Mediterranean ecosystems: Model calibration using
607 the Bayesian approach. Agriculture Ecosystems & Environment, 161, 88-100. doi:10.1016/j.agee.2012.07.025
608 Cuezva, S., Fernandez-Cortes, A., Benavente, D., Serrano-Ortiz, R., Kowalski, A. S., & Sanchez-Moral, S. (2011).
609 Short-term CO2(g) exchange between a shallow karstic cavity and the external atmosphere during summer: Role
610 of the surface soil layer. Atmospheric Environment, 45(7), 1418-1427.
611 Davidson, E. A., & Janssens, I. A. (2006). Temperature sensitivity of soil carbon decomposition and feedbacks to
612 climate change. Nature, 440(7081), 165-173.
613 Davidson, E. A., Belk, E., & Boone, R. D. (1998). Soil water content and temperature as independent or confounded
614 factors controlling soil respiration in a temperate mixed hardwood forest. Global Change Biology, 4(2), 217-227.
615 DeLucia, E. H., Drake, J. E., Thomas, R. B., & Gonzalez-Meler, M. (2007). Forest carbon use efficiency: is respiration
616 a constant fraction of gross primary production? Global Change Biology, 13(6), 1157-1167.
617 Deng, Q., Hui, D., Zhang, D., Zhou, G., Liu, J., Liu, S., et al. (2012). Effects of Precipitation Increase on Soil
618 Respiration: A Three-Year Field Experiment in Subtropical Forests in China. Plos One, 7(7).
619 Dirks, I., Navon, Y., Kanas, D., Dumbur, R., & Grunzweig, J. M. (2010). Atmospheric water vapor as driver of litter
620 decomposition in Mediterranean shrubland and grassland during rainless seasons. Global Change Biology,
621 16(10), 2799-2812. doi:10.1111/j.1365-2486.2010.02172.x
622 Eshel, G., Fine, P., & Singer, M. J. (2007). Total soil carbon and water quality: An implication for carbon
623 sequestration. Soil Science Society of America Journal, 71(2), 397-405. doi:10.2136/sssaj2006.0061
624 Falge, E., Baldocchi, D., Tenhunen, J., Aubinet, M., Bakwin, P., Berbigier, P., et al. (2002). Seasonality of ecosystem
625 respiration and gross primary production as derived from FLUXNET measurements. Agricultural and Forest
626 Meteorology, 113(1-4), 53-74.
627 Frank, A. B., Liebig, M. A., & Hanson, J. D. (2002). Soil carbon dioxide fluxes in northern semiarid grasslands. Soil
628 Biology & Biochemistry, 34(9), 1235-1241.
629 Frey, B., Hagedorn, F., & Giudici, F. (2006). Effect of girdling on soil respiration and root composition in a sweet
630 chestnut forest. Forest Ecology and Management, 225(1-3), 271-277.
631 Giardina, C. P., & Ryan, M. G. (2002). Total belowground carbon allocation in a fast-growing Eucalyptus plantation
632 estimated using a carbon balance approach. Ecosystems, 5(5), 487-499.
633 Gliksman, D., Rey, A., Seligmann, R., Dumbur, R., Sperling, O., Navon, Y., . . . Grunzweig, J. M. (2017). Biotic
634 degradation at night, abiotic degradation at day: positive feedbacks on litter decomposition in drylands. Global
635 Change Biology, 23(4), 1564-1574. doi:10.1111/gcb.13465
636 Graven, H. D., Guilderson, T. P., & Keeling, R. F. (2012). Observations of radiocarbon in CO2 at La Jolla, California,
637 USA 1992-2007: Analysis of the long-term trend. Journal of Geophysical Research-Atmospheres, 117.
638 Grünzweig, J. M., Gelfand, I., Fried, Y., & Yakir, D. (2007). Biogeochemical factors contributing to enhanced carbon
639 storage following afforestation of a semi-arid shrubland. Biogeosciences, 4(5), 891-904.
640 Grünzweig, J. M., Hemming, D., Maseyk, K., Lin, T., Rotenberg, E., Raz-Yaseef, N., et al. (2009). Water limitation

https://doi.org/10.5194/bg-2019-291
Preprint. Discussion started: 31 July 2019

to soil CO2 efflux in a pine forest at the semiarid "timberline". Journal of Geophysical Research-Biogeosciences, 114.

Grünzweig, J. M., Lin, T., Rotenberg, E., Schwartz, A., & Yakir, D. (2003). Carbon sequestration in arid-land forest. Global Change Biology, 9(5), 791-799.

Hashimoto, S., Carvalhais, N., Ito, A., Migliavacca, M., Nishina, K., & Reichstein, M. (2015). Global spatiotemporal distribution of soil respiration modeled using a global database. Biogeosciences, 12(13), 4121-4132.

Heinemeyer, A., Hartley, I. P., Evans, S. P., De la Fuente, J. A. C., & Ineson, P. (2007). Forest soil CO2 flux: uncovering the contribution and environmental responses of ectomycorrhizas. Global Change Biology, 13(8), 1786-1797.

Hemming, D., Yakir, D., Ambus, P., Aurela, M., Besson, C., Black, K., . . . Vesala, T. (2005). Pan-European delta C-13 values of air and organic matter from forest ecosystems. Global Change Biology, 11(7), 1065-1093. doi:10.1111/j.1365-2486.2005.00971.x

Hogberg, P., Bhupinderpal, S., Lofvenius, M. O., & Nordgren, A. (2009). Partitioning of soil respiration into its autotrophic and heterotrophic components by means of tree-girdling in old boreal spruce forest. Forest Ecology and Management, 257(8), 1764-1767.

Hui, D. F., & Luo, Y. Q. (2004). Evaluation of soil CO2 production and transport in Duke Forest using a process-based modeling approach. Global Biogeochemical Cycles, 18(4).

IPCC, (2014). Climate Change 2014: Mitigation of Climate Change. Contribution of Working Group III to the Fifth Assessment Report of the Intergovernmental Panel on Climate Change [Edenhofer, O., R. et al.]. Cambridge University Press, Cambridge and New York.

Jiang, H., Deng, Q., Zhou, G., Hui, D., Zhang, D., Liu, S., et al. (2013). Responses of soil respiration and its temperature/moisture sensitivity to precipitation in three subtropical forests in southern China. Biogeosciences, 10(6), 3963-3982.

Johnsen, K., Maier, C., Sanchez, F., Anderson, P., Butnor, J., Waring, R., et al. (2007). Physiological girdling of pine trees via phloem chilling: proof of concept. Plant Cell and Environment, 30(1), 128-134.

Kappen, L., Lange, O. L., Schulze, E. D., Evenari, M., & Buschbom, U. (1979). ECOPHYSIOLOGICAL INVESTIGATIONS ON LICHENS OF THE NEGEV DESERT .6. ANNUAL COURSE OF THE PHOTOSYNTHETIC PRODUCTION OF RAMALINA-MACIFORMIS (DEL) BORY. Flora, 168(1-2), 85-108.

Köchy, M., Hiederer, R., & Freibauer, A. (2015). Global distribution of soil organic carbon - Part 1: Masses and frequency distributions of SOC stocks for the tropics, permafrost regions, wetlands, and the world. Soil, 1(1), 351-365.

Kosmas, C., Danalatos, N. G., Poesen, J., & van Wesemael, B. (1998). The effect of water vapour adsorption on soil moisture content under Mediterranean climatic conditions. Agricultural Water Management, 36(2), 157-168. doi:10.1016/s0378-3774(97)00050-4

Kowalski, A. S., Serrano-Ortiz, P., Janssens, I. A., Sanchez-Moral, S., Cuezva, S., Domingo, F., et al. (2008). Can flux tower research neglect geochemical CO2 exchange? Agricultural and Forest Meteorology, 148(6-7), 1045-1054.

Kuehn, K. A., Steiner, D., & Gessner, M. O. (2004). Diel mineralization patterns of standing-dead plant litter: Implications for CO2 flux from wetlands. Ecology, 85(9), 2504-2518. doi:10.1890/03-4082

Kuzyakov, Y. (2006). Sources of CO2 efflux from soil and review of partitioning methods. [Review]. Soil Biology & Biochemistry, 38(3), 425-448.

Lange, O. L., Green, T. G. A., Melzer, B., Meyer, A., & Zellner, H. (2006). Water relations and CO2 exchange of the terrestrial lichen Teloschistes capensis in the Namib fog desert: Measurements during two seasons in the field and under controlled conditions. Flora, 201(4), 268-280. doi:10.1016/j.flora.2005.08.003

Le Quéré, C., Andrew, R. M., Friedlingstein, P., Sitch, S., Pongratz, J., Manning, A. C., et al. (2018). Global Carbon Budget 2017. Earth System Science Data, 10(1), 405-448.

Lellei-Kovacs, E., Kovacs-Lang, E., Botta-Dukat, Z., Kalapos, T., Emmett, B., & Beier, C. (2011). Thresholds and interactive effects of soil moisture on the temperature response of soil respiration. European Journal of Soil Biology, 47(4), 247-255.

Levin, I., Naegler, T., Kromer, B., Diehl, M., Francey, R. J., Gomez-Pelaez, A. J., et al. (2010). Observations and modelling of the global distribution and long-term trend of atmospheric (CO2)-C-14 (vol 62, pg 26, 2010). Tellus Series B-Chemical and Physical Meteorology, 62(3), 207-207.

Lin, G. H., Ehleringer, J. R., Rygiewicz, P. T., Johnson, M. G., & Tingey, D. T. (1999). Elevated CO2 and temperature impacts on different components of soil CO2 efflux in Douglas-fir terracosms. Global Change Biology, 5(2), 157-168.

Litton, C. M., Raich, J. W., & Ryan, M. G. (2007). Carbon allocation in forest ecosystems. Global Change Biology, 13(10), 2089-2109.

https://doi.org/10.5194/bg-2019-291
Preprint. Discussion started: 31 July 2019

699 Litton, C. M., Ryan, M. G., & Knight, D. H. (2004). Effects of tree density and stand age on carbon allocation patterns
700 in postfire lodgepole pine. Ecological Applications, 14(2), 460-475. doi:10.1890/02-5291
701 Lopez-Ballesteros, A., Serrano-Ortiz, P., Kowalski, A. S., Sanchez-Canete, E. P., Scott, R. L., & Domingo, F. (2017).
702 Subterranean ventilation of allochthonous CO2 governs net CO2 exchange in a semiarid Mediterranean
703 grassland. Agricultural and Forest Meteorology, 234, 115-126. doi:10.1016/j.agrformet.2016.12.021
704 Maseyk, K. S., Lin, T., Rotenberg, E., Gruenzweig, J. M., Schwartz, A., & Yakir, D. (2008b). Physiology-phenology
705 interactions in a productive semi-arid pine forest. New Phytologist, 178(3), 603-616.
706 Maseyk, K., Grünzweig, J. M., Rotenberg, E., & Yakir, D. (2008a). Respiration acclimation contributes to high
707 carbon-use efficiency in a seasonally dry pine forest. Global Change Biology, 14(7), 1553-1567.
708 Maseyk, K., Hemming, D., Angert, A., Leavitt, S. W., & Yakir, D. (2011). Increase in water-use efficiency and
709 underlying processes in pine forests across a precipitation gradient in the dry Mediterranean region over the past
710 30 years. Oecologia, 167(2), 573-585. doi:10.1007/s00442-011-2010-4
711 Matteucci, M., Gruening, C., Ballarin, I. G., & Cescatti, A. (2014). Soil and ecosystem carbon fluxes in a
712 Mediterranean forest during and after drought. Agrochimica, 58, 91-115.
713 Matteucci, M., Gruening, C., Ballarin, I. G., Seufert, G., & Cescatti, A. (2015). Components, drivers and temporal
714 dynamics of ecosystem respiration in a Mediterranean pine forest. Soil Biology & Biochemistry, 88, 224-235.
715 doi:10.1016/j.soilbio.2015.05.017
716 Newell, S. Y., Fallon, R. D., Rodriguez, R. M. C., & Groene, L. C. (1985). INFLUENCE OF RAIN, TIDAL
717 WETTING AND RELATIVE-HUMIDITY ON RELEASE OF CARBON-DIOXIDE BY STANDING-DEAD
718 SALT-MARSH PLANTS. Oecologia, 68(1), 73-79. doi:10.1007/bf00379477
719 Noh, N. J., Son, Y., Lee, S. K., Yoon, T. K., Seo, K. W., Kim, C., . . . Hwang, J. (2010). Influence of stand density
720 on soil CO2 efflux for a Pinus densiflora forest in Korea. Journal of Plant Research, 123(4), 411-419.
721 doi:10.1007/s10265-010-0331-8
722 Ogee, J., Peylin, P., Cuntz, M., Bariac, T., Brunet, Y., Berbigier, P., et al. (2004). Partitioning net ecosystem carbon
723 exchange into net assimilation and respiration with canopy-scale isotopic measurements: An error propagation
724 analysis with (CO2)-C-13 and (COO)-O-18 data. Global Biogeochemical Cycles, 18(2).
725 Olsson, P., Linder, S., Giesler, R., & Hogberg, P. (2005). Fertilization of boreal forest reduces both autotrophic and
726 heterotrophic soil respiration. Global Change Biology, 11(10), 1745-1753.
727 Pataki, D. E., Ehleringer, J. R., Flanagan, L. B., Yakir, D., Bowling, D. R., Still, C. J., et al. (2003). The application
728 and interpretation of Keeling plots in terrestrial carbon cycle research. Global Biogeochemical Cycles, 17(1).
729 Peterjohn, W. T., Melillo, J. M., Steudler, P. A., Newkirk, K. M., Bowles, F. P., & Aber, J. D. (1994). RESPONSES
730 OF TRACE GAS FLUXES AND N AVAILABILITY TO EXPERIMENTALLY ELEVATED SOIL
731 TEMPERATURES. Ecological Applications, 4(3), 617-625.
732 Poulter, B., Frank, D., Ciais, P., Myneni, R. B., Andela, N., Bi, J., et al. (2014). Contribution of semi-arid ecosystems
733 to interannual variability of the global carbon cycle. Nature, 509(7502), 600-+.
734 Raich, J. W., & Schlesinger, W. H. (1992). THE GLOBAL CARBON-DIOXIDE FLUX IN SOIL RESPIRATION
735 AND ITS RELATIONSHIP TO VEGETATION AND CLIMATE. Tellus Series B-Chemical and Physical
736 Meteorology, 44(2), 81-99.
737 Raz-Yaseef, N., Rotenberg, E., & Yakir, D. (2010). Effects of spatial variations in soil evaporation caused by tree
738 shading on water flux partitioning in a semi-arid pine forest. Agricultural and Forest Meteorology, 150(3), 454-
739 462.
740 Reichstein, M., Rey, A., Freibauer, A., Tenhunen, J., Valentini, R., Banza, J., et al. (2003). Modeling temporal and
741 large-scale spatial variability of soil respiration from soil water availability, temperature and vegetation
742 productivity indices. Global Biogeochemical Cycles, 17(4).
743 Rey, A., Pegoraro, E., Tedeschi, V., De Parri, I., Jarvis, P. G., & Valentini, R. (2002). Annual variation in soil
744 respiration and its components in a coppice oak forest in Central Italy. Global Change Biology, 8(9), 851-866.
745 Roland, M., et al. (2012). Contributions of carbonate weathering to the net ecosystem carbon balance of a
746 mediterranean forest. Thesis submitted to Antwerpen University, Antwerpen, Belgium.
747 Ross, I., Misson, L., Rambal, S., Arneth, A., Scott, R. L., Carrara, A., et al. (2012). How do variations in the temporal
748 distribution of rainfall events affect ecosystem fluxes in seasonally water-limited Northern Hemisphere
749 shrublands and forests? Biogeosciences, 9(3), 1007-1024.
750 Rotenberg, E., & Yakir, D. (2010). Contribution of Semi-Arid Forests to the Climate System. Science, 327(5964),
751 451-454.
752 Ryan, M. G. (1991). EFFECTS OF CLIMATE CHANGE ON PLANT RESPIRATION. Ecological Applications,
753 1(2), 157-167.
754 Ryan, M. G., & Law, B. E. (2005). Interpreting, measuring, and modeling soil respiration. [Article]. Biogeochemistry,
755 73(1), 3-27.
756 Saleska, S. R., Harte, J., & Torn, M. S. (1999). The effect of experimental ecosystem warming on CO2 fluxes in a

https://doi.org/10.5194/bg-2019-291
Preprint. Discussion started: 31 July 2019

montane meadow. Global Change Biology, 5(2), 125-141.
Scharlemann, J. P. W., Tanner, E. V. J., Hiederer, R., & Kapos, V. (2014). Global soil carbon: understanding and managing the largest terrestrial carbon pool. Carbon Management, 5(1), 81-91.
Schiller, G. (2000), Ecophysiology of Pinus halepensis Mill. and P. brutia Ten, in Ecology, Biogeography and Management of Pinus halepensis and P. brutia Forest Ecosystems in the Mediterranean Basin, edited by G. Ne'eman and L. Trabaud, pp. 51–65, Backhuys, Leiden, Netherlands.
Schlesinger, W. H. (1982). CARBON STORAGE IN THE CALICHE OF ARID SOILS - A CASE-STUDY FROM ARIZONA. Soil Science, 133(4), 247-255.
Schulze, E. D. (2006). Biological control of the terrestrial carbon sink. Biogeosciences, 3(2), 147-166.
Serrano-Ortiz, P., Roland, M., Sanchez-Moral, S., Janssens, I. A., Domingo, F., Godderis, Y., & Kowalski, A. S. (2010). Hidden, abiotic CO2 flows and gaseous reservoirs in the terrestrial carbon cycle: Review and perspectives. Agricultural and Forest Meteorology, 150(3), 321-329. doi:10.1016/j.agrformet.2010.01.002
Shachnovich, Y., Berliner, P. R., & Bar, P. (2008). Rainfall interception and spatial distribution of throughfall in a pine forest planted in an arid zone. Journal of Hydrology, 349(1-2), 168-177.
Shen, W. J., Jenerette, G. D., Hui, D. F., Phillips, R. P., & Ren, H. (2008). Effects of changing precipitation regimes on dryland soil respiration and C pool dynamics at rainfall event, seasonal and interannual scales. Journal of Geophysical Research-Biogeosciences, 113(G3).
Subke, J.-A., Voke, N. R., Leronni, V., Garnett, M. H., & Ineson, P. (2011). Dynamics and pathways of autotrophic and heterotrophic soil CO2 efflux revealed by forest girdling. Journal of Ecology, 99(1), 186-193.
Taneva, L., & Gonzalez-Meler, M. A. (2011). Distinct patterns in the diurnal and seasonal variability in four components of soil respiration in a temperate forest under free-air CO2 enrichment. Biogeosciences, 8(10), 3077-3092.
Tang, J. W., Baldocchi, D. D., & Xu, L. (2005). Tree photosynthesis modulates soil respiration on a diurnal time scale. Global Change Biology, 11(8), 1298-1304.
Tatarinov, F., Rotenberg, E., Maseyk, K., Ogee, J., Klein, T., & Yakir, D. (2016). Resilience to seasonal heat wave episodes in a Mediterranean pine forest. New Phytologist, 210(2), 485-496.
Taylor, A. J., Lai, C. T., Hopkins, F. M., Wharton, S., Bible, K., Xu, X. M., et al. (2015). Radiocarbon-Based Partitioning of Soil Respiration in an Old-Growth Coniferous Forest. Ecosystems, 18(3), 459-470.
Villegas, J. C., Dominguez, F., Barron-Gafford, G. A., Adams, H. D., Guardiola-Claramonte, M., Sommer, E. D., . . . Huxman, T. E. (2015). Sensitivity of regional evapotranspiration partitioning to variation in woody plant cover: insights from experimental dryland tree mosaics. Global Ecology and Biogeography, 24(9), 1040-1048. doi:10.1111/geb.12349
Volcani, A., Karnieli, A., & Svoray, T. (2005). The use of remote sensing and GIS for spatio-temporal analysis of the physiological state of a semi-arid forest with respect to drought years. Forest Ecology and Management, 215(1-3), 239-250. doi:10.1016/j.foreco.2005.05.063
Xu, M., & Qi, Y. (2001). Soil-surface CO2 efflux and its spatial and temporal variations in a young ponderosa pine plantation in northern California. Global Change Biology, 7(6), 667-677.
Xu, Z. F., Tang, S. S., Xiong, L., Yang, W. Q., Yin, H. J., Tu, L. H., . . . Tan, B. (2015). Temperature sensitivity of soil respiration in China's forest ecosystems: Patterns and controls. Applied Soil Ecology, 93, 105-110. doi:10.1016/j.apsoil.2015.04.008
Yakir, D., & Sternberg, L. D. L. (2000). The use of stable isotopes to study ecosystem gas exchange. Oecologia, 123(3), 297-311.
Yu, S. Q., Chen, Y. Q., Zhao, J., Fu, S. L., Li, Z., Xia, H. P., & Zhou, L. X. (2017). Temperature sensitivity of total soil respiration and its heterotrophic and autotrophic components in six vegetation types of subtropical China. Science of the Total Environment, 607, 160-167. doi:10.1016/j.scitotenv.2017.06.194
Zhao, Z. Y., Peng, C. H., Yang, Q., Meng, F. R., Song, X. Z., Chen, S. T., et al. (2017). Model prediction of biome-specific global soil respiration from 1960 to 2012. Earths Future, 5(7), 715-729.
Zhou, T., Shi, P. J., Hui, D. F., & Luo, Y. Q. (2009). Global pattern of temperature sensitivity of soil heterotrophic respiration (Q(10)) and its implications for carbon-climate feedback. Journal of Geophysical Research-Biogeosciences, 114.